一般社団法人　電子情報通信学会
THE INSTITUTE OF ELECTRONICS,
INFORMATION AND COMMUNICATION ENGINEERS

信学技報
IEICE Technical Report
RCS2015-338(2016-03)

# Low-PAPR Filtered Single Carrier Signal Transmission with Space-Time Transmit Diversity and Blind Time-Domain Selected Mapping

Amnart Boonkajay† and Fumiyuki Adachi‡

†‡Department of Communications Engineering, Graduate School of Engineering, Tohoku University
6-6-05 Aza-Aoba, Aramaki, Aoba-ku, Sendai, Miyagi, 980-8579 Japan
E-mail: †amnart@mobile.ecei.tohoku.ac.jp ‡adachi@ecei.tohoku.ac.jp

**Abstract** Single-carrier with frequency-domain equalization (SC-FDE) is a promising transmission technique obtaining frequency diversity gain with low peak-to-average power ratio (PAPR) property. The use of space-time block coded transmit diversity (STTD) utilizes multi-antenna transmission to improve the transmission quality. PAPR can be further reduced without degrading other performances by employing a blind time-domain selected mapping (blind TD-SLM). The blind TD-SLM requires no side-information sharing and hence, does not cause any spectrum efficiency (SE) degradation. In this paper, we propose a low-PAPR filtered SC-FDE transmission using STTD and blind TD-SLM. STTD is carried out by employing a simple orthogonal space-time block coding (STBC), where the blind TD-SLM uses polyphase rotations. It is also shown in this paper that the blind TD-SLM can be implemented by applying phase rotation to time-domain transmit block before STTD encoding. Performance evaluation of low-PAPR SC-FDE with STTD and blind TD-SLM is done by computer simulation in aspects of PAPR and bit-error rate (BER). It is confirmed that the PAPR can be reduced without significant degradation of BER performance and without side-information sharing.

**Keyword** Space-time transmit diversity (STTD), Single-carrier (SC) transmission, peak-to-average power ratio (PAPR), selected mapping (SLM), frequency-domain equalization (FDE)

## 1. Introduction

Small-cell network using distributed antennas (DA) [1] is a promising candidate for the fifth-generation (5G) mobile communication systems as it achieves high spectrum efficiency (SE) and energy efficiency (EE) simultaneously. Space-time block coded transmit diversity (STTD) [2] is a cooperative multi-input multi-output (MIMO) [3] transmission technique utilizing the DAs to acquire spatial diversity gain, and hence improves SE of user equipment (UE). The use of STTD and single-carrier with frequency-domain equalization (SC-FDE) [4] is very attractive for uplink transmission due to the following reason. SC-FDE transmission is robust against fading [5], while its waveform has low peak-to-average power ratio (PAPR). The low-PAPR transmit waveform contributes to low input power into transmit power amplifier (PA), resulting in low power consumption in the PA.

SC-FDE needs to equip with transmit filtering for limiting transmission bandwidth [6]. The PAPR of filtered SC-FDE signal, however, becomes higher when higher data modulation level is used [7]. To deal with a problem of high-PAPR signal, a PAPR reduction technique based on phase rotation called selected mapping (SLM) [8] can be considered as a promising solution. SLM can effectively reduce the PAPR without signal distortion but with small overhead bits. The authors recently proposed SLM techniques for filtered SC-FDE (or discrete Fourier transform (DFT)-precoded OFDM) signal, in which the phase rotation is applied either in frequency domain (called FD-SLM) [9] or in time domain (called TD-SLM) [10]. Furthermore, the authors proposed blind SLM which does not require transmission of side-information for FD-SLM and TD-SLM [9-10].

Similar to single-antenna case, SC-FDE using STTD experiences the problem of high-PAPR signal when the transmit filtering and higher-level data modulation are applied. The authors examined this problem in [11] and proposed a blind FD-SLM for STTD. The proposed blind FD-SLM in [11] can reduce the PAPR, however, the PAPR is still higher than that of single-antenna case because of the use of common phase rotation pattern. Meanwhile, an extension of blind TD-SLM to filtered SC-FDE using STTD has not been yet studied.

In this paper, a low-PAPR filtered SC-FDE transmission using STTD and blind TD-SLM is proposed. STTD employs a simple orthogonal space-time block coding (STBC) and the blind TD-SLM uses polyphase rotations. It is also shown in this paper that the blind TD-SLM can be implemented by multiplying the phase rotation pattern to the time-domain transmit block before STTD encoding, which requires less computation times for transmit waveform candidate generation and PAPR calculation compared to [11]. Performance evaluation of low-PAPR filtered SC-FDE with STTD and blind TD-SLM is done by computer simulation in terms of PAPR and bit-error rate (BER). Simulation results show that the blind TD-SLM can effectively reduce the PAPR without causing a significant BER performance degradation.

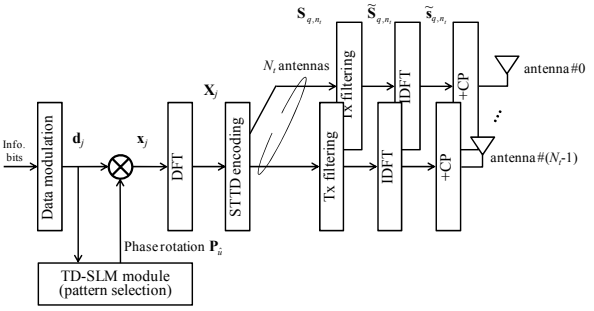


**Fig.1** Transmitter.

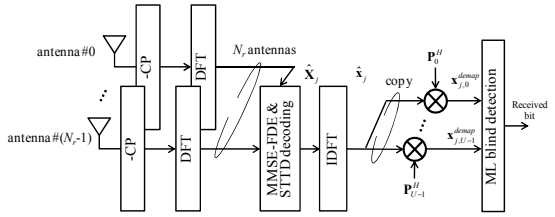


**Fig.2** Receiver

**Table 1** Relationship of $N_t$, $J$, $Q$ and STBC coding rate.

| $N_t$ | $J$ | $Q$ | $R_{\mathrm{STBC}}=J/Q$ |
|---|---|---|---|
| 1 | 1 | 1 | 1 |
| 2 | 2 | 2 | 1 |
| 3 | 3 | 4 | 3/4 |
| 4 | 3 | 4 | 3/4 |

## 2. Transmitter system model

The transmitter system model of low-PAPR filtered SC-FDE using STTD and blind TD-SLM is illustrated by Fig. 1. For simplicity, point-to-point transmission using $N_t$ transmit antennas and $N_r$ receive antennas is assumed in this paper. Block transmission is assumed, where the transmit signal and processing techniques are represented by row vector and matrices, respectively. It is also observed in Fig. 1 that the phase rotation is applied prior to DFT operation and STTD encoding.

### 2.1. Transmitter

We begin with $J$ blocks of $N_c$-length data-modulated transmit vector $\mathbf{d}=[\mathbf{d}_0,\mathbf{d}_1,...,\mathbf{d}_{J-1}]^T$, $j$=0~$J$−1 where $\mathbf{d}_j=[d_j(0),d_j(1),\ldots,d_j(N_c-1)]^T$. The transmit blocks are then phase rotated by phase rotation matrix $\mathbf{P}_{\hat{u}}$, yielding the phase-rotated time-domain signal $\mathbf{x}=\mathbf{P}_{\hat{u}}\mathbf{d}$, where $\mathbf{x}=[\mathbf{x}_0,\mathbf{x}_1,...,\mathbf{x}_{J-1}]^T$ and $j$=0~$J$−1. The phase rotation matrix $\mathbf{P}_{\hat{u}}$ is a $JN_c\times JN_c$ diagonal matrix consisting of a selected phase rotation pattern for each block $\mathbf{d}_j$, which is

$$\mathbf{P}_{\hat{u}}=\begin{bmatrix}\mathbf{P}_{\hat{u},0} & & & \mathbf{0}\\ & \mathbf{P}_{\hat{u},1} & & \\ & & \ddots & \\ \mathbf{0} & & & \mathbf{P}_{\hat{u},J-1}\end{bmatrix}, \tag{1}$$

where $\hat{u},j$ represents the selected phase rotation pattern index for the $j$-th block. The method of finding the phase rotation providing the lowest PAPR $\mathbf{P}_{\hat{u},j}$ will be described in Subsection 2.2.

Next, the $j$-th transmit block $\mathbf{x}_j$ is transformed into frequency domain by $N_c$-point DFT, yielding the $j$-th block of frequency signal $\mathbf{X}_j=[X_j(0),X_j(1),...,X_j(N_c-1)]^T$ as $\mathbf{X}_j=\mathbf{F}_{N_c}\mathbf{x}_j$, where $\mathbf{F}_{N_c}$ is expressed by

$$\mathbf{F}_{N_c}=\frac{1}{\sqrt{N_c}}\begin{bmatrix}1 & 1 & \cdots & 1\\ 1 & e^{\frac{-j2\pi(1)(1)}{N_c}} & \cdots & e^{\frac{-j2\pi(1)(N_c-1)}{N_c}}\\ \vdots & \vdots & \ddots & \vdots\\ 1 & e^{\frac{-j2\pi(N_c-1)(1)}{N_c}} & \cdots & e^{\frac{-j2\pi(N_c-1)(N_c-1)}{N_c}}\end{bmatrix}, \tag{2}$$

and its Hermitian transpose $\mathbf{F}_{N_c}^H$ represents inverse DFT (IDFT) operation.

After that, $J$ blocks of frequency-domain signal $\mathbf{X}_j$ are encoded by STTD encoding, which is same as orthogonal STBC [2], then obtaining $N_t$ parallel streams of $Q$ blocks $\mathbf{S}_{N_t}=[\mathbf{S}_0,...,\mathbf{S}_q,...,\mathbf{S}_{Q-1}]$ where $\mathbf{S}_q=[\mathbf{S}_{q,0},...,\mathbf{S}_{q,n_t},...,\mathbf{S}_{q,N_t-1}]^T$. The STTD-encoded blocks $\mathbf{S}_{N_t}$ depend on $N_t$ and is expressed by [12]

$$\mathbf{S}_{N_t=1}=\mathbf{X}_0, \tag{3a}$$

$$\mathbf{S}_{N_t=2}=\begin{bmatrix}\mathbf{X}_0 & -\mathbf{X}_1^*\\ \mathbf{X}_1 & \mathbf{X}_0^*\end{bmatrix}, \tag{3b}$$

$$\mathbf{S}_{N_t=3}=\begin{bmatrix}\mathbf{X}_0 & -\mathbf{X}_1^* & -\mathbf{X}_2^* & \mathbf{0}\\ \mathbf{X}_1 & \mathbf{X}_0^* & \mathbf{0} & -\mathbf{X}_2^*\\ \mathbf{X}_2 & \mathbf{0} & \mathbf{X}_0^* & \mathbf{X}_1^*\end{bmatrix}, \tag{3c}$$

$$\mathbf{S}_{N_t=4}=\begin{bmatrix}\mathbf{X}_0 & -\mathbf{X}_1^* & -\mathbf{X}_2^* & \mathbf{0}\\ \mathbf{X}_1 & \mathbf{X}_0^* & \mathbf{0} & -\mathbf{X}_2^*\\ \mathbf{X}_2 & \mathbf{0} & \mathbf{X}_0^* & \mathbf{X}_1^*\\ \mathbf{0} & \mathbf{X}_2 & -\mathbf{X}_1 & \mathbf{X}_0\end{bmatrix}. \tag{3d}$$

In addition, the relationship between $J$ and $Q$, and the corresponding coding rate $R_{\mathrm{STBC}}=J/Q$, is shown in Table 1.

Transmit filtering matrix $\mathbf{H}_T=diag[H_T(0),...,H_T(N_c-1)]$, are multiplied to all encoded transmit blocks in frequency domain for limiting transmission bandwidth. The transmit filtering is assumed to be square-root raised cosine (SRRC) filtering with roll-off factor $\alpha$=0 in this paper. After that, $\widetilde{\mathbf{S}}_{q,n_t}\ q=0\sim Q-1, n_t=0\sim N_t-1$ is expressed by

$$\widetilde{\mathbf{S}}_{q,n_t}=\mathbf{H}_T\mathbf{S}_{q,n_t}. \tag{4}$$

After that, $\widetilde{\mathbf{S}}_{q,n_t}$ is transformed back into time domain by $N_c$-point IDFT, yielding the $q$-th time-domain transmit block at the $n_t$-th antenna $\widetilde{\mathbf{s}}_{q,n_t}=\mathbf{F}_{N_c}^H\widetilde{\mathbf{S}}_{q,n_t}$. Finally, the last $N_g$ samples of transmit block are copied as a cyclic prefix (CP) and inserted into the guard interval (GI), then a CP-inserted signal block of $N_g$+$N_c$ samples is transmitted.

### 2.2. TD-SLM algorithm

Assuming that an $N_c$-length time-domain transmit block is represented by $\mathbf{s}=[s(0),s(1),\ldots,s(N_c-1)]^T$, PAPR is calculated over an oversampled block, which is

$$\mathrm{PAPR}(\mathbf{s}) = \frac{\max\{|s(n)|^2, n = 0, \frac{1}{V}, \frac{2}{V}, ..., N_c - 1\}}{\frac{1}{N_c}\sum_{n=0}^{N_c-1}|s(n)|^2}, \quad (5)$$

where $V$ represents oversampling factor. In case of multi-antenna transmission, the PAPR is calculated from the transmit waveform of each transmit antenna.

Since the PAPR of complex-conjugated version of frequency-domain signal is exactly the same as the original signal, we can reduce the number of blocks needed to consider in TD-SLM per one STTD encoding time from $N_t \times Q$ blocks to $J$ blocks. In other words, finding the phase rotation pattern which minimizes the PAPR of $\mathbf{d}_j, j = 0 \sim J-1$ is equivalent to finding the phase rotation pattern for minimizing the PAPR of transmit blocks $\widetilde{\mathbf{s}}_{q,n_t}, q = 0 \sim Q-1, n_t = 0 \sim N_t - 1$ . The above discussion confirms that applying the phase rotation before STTD encoding yields the same PAPR performance compared to that of applying phase rotation after STTD encoding.

A set of $U$ different $N_c \times N_c$ diagonal polyphase rotation pattern matrices $\mathbf{P}_u = diag[P_u(0), \ldots, P_u(N_c-1)]$, $u = 0 \sim U-1$ is defined in random approach as $P_u(n) \in \{e^{j0}, e^{j(2\pi/3)}, e^{-j(2\pi/3)}\}$, $n = 0 \sim N_c - 1$, except the first rotation pattern is an identity matrix $\mathbf{I}_{N_c}$ . The above polyphase rotations are defined by referring [10] as a sufficient condition in order to allow the blind TD-SLM. The selection criteria of phase rotation pattern $\mathbf{P}_{\hat{u},j}, j = 0 \sim J-1$ can be described into 2 categories; minimizing the maximum PAPR of all $J$ time-domain transmit blocks (hereinafter called minimax criterion) and minimizing the PAPR of each time-domain transmit block $\mathbf{d}_j$. The selection based on minimax criterion selects only one common phase rotation pattern for all $J$ blocks and is expressed by the following equation.

$$\mathbf{P}_{\hat{u},j} = \arg \min_{u=0,1,\ldots,U-1} \left( \max_{j=0,1,\ldots,J-1} (\mathrm{PAPR}(\mathbf{F}_{N_c}^H \mathbf{H}_T \mathbf{F}_{N_c} \mathbf{P}_{u,j} \mathbf{d}_j)) \right). \quad (6)$$

From (6), it can be observed that the selected phase rotation pattern $\mathbf{P}_{\hat{u},j}$ is identical for all $j = 0 \sim J-1$. The use of common phase rotation pattern for all $J$ transmit blocks has been discussed in [11] and assuming FD-SLM that it can preserve STTD code orthogonality. However, the minimax criterion decreases degree of freedom and hence increases the PAPR compared to single-antenna transmission.

On the other hand, a selection criterion based on minimizing the PAPR of each time-domain transmit block $\mathbf{d}_j$, $j = 0 \sim N_c - 1$, is expressed by the following equation.

$$\mathbf{P}_{\hat{u},j} = \arg \min_{u=0,1,\ldots,U-1} (\mathrm{PAPR}(\mathbf{F}_{N_c}^H \mathbf{H}_T \mathbf{F}_{N_c} \mathbf{P}_{u,j} \mathbf{d}_j)). \quad (7)$$

In (7), $\mathbf{P}_{\hat{u},j}$ can be different for $j = 0 \sim J-1$, resulting in the same degree of freedom compared to single-antenna transmission. Therefore, the PAPR of TD-SLM using the selected criterion in (7) is expected to be the same as that of TD-SLM in single-antenna case [10]. Moreover, it can be seen from (1), (3) and (7) that the phase rotation is applied before STTD encoding, which means the TD-SLM and STTD encoding are independent to each other, and consequently the use of selection criterion in (7) does not violate the STTD code orthogonality.

## 3. Receiver system model

The receiver system model of low-PAPR filtered SC-FDE using STTD and blind TD-SLM is illustrated by Fig. 2. It can be seen that the receiver consists of two main processes; joint FDE based on minimum mean-square error (MMSE-FDE) and STTD decoding, and joint blind phase rotation pattern estimation & data detection for TD-SLM, which are described in Subsection 3.1 and 3.2, respectively.

### 3.1. Joint MMSE-FDE and STTD decoding

The wireless propagation channel is assumed to be a symbol-spaced $L$-path frequency-selective block Rayleigh fading channel [5], where its impulse response between the $n_t$-th transmit antenna and the $n_r$-th distributed antenna (i.e. received antenna) is given by

$$h_{n_r,n_t}(\tau) = \sum_{l=0}^{L-1} h_{n_r,n_t,l}\, \delta(\tau - \tau_{n_r,n_t,l}), \quad (8)$$

where $h_{n_r,n_t,l}$ and $\tau_{n_r,n_t,l}$ are complex-valued path gain and time delay of the $l$-th path, respectively. In addition, $h_{n_r,n_t,l}$ is assumed to be the same for $Q$ encoded block in this paper for simplicity.

The $q$-th block discrete-time received signal at the $n_r$-th distributed antenna $\mathbf{r}_{q,n_r} = [r_{q,n_r}(0), r_{q,n_r}(1), \ldots, r_{q,n_r}(N_c-1)]^T$ can be expressed by

$$r_{q,n_r}(n) = \sqrt{\frac{2E_s}{T_s}} \sum_{n_t=0}^{N_t-1} \sum_{l=0}^{L-1} h_{n_r,n_t,l}\, \widetilde{s}_{\hat{u},q,n_t}(n - \tau_{n_r,n_t,l}) + z_{q,n_r}(n), \quad (9)$$

where $z_{q,n_r}(n)$ is an additive white Gaussian noise (AWGN) having zero mean and the variance of $2N_0/T_s$ with $T_s$ is symbol duration and $N_0$ being the one-sided noise power spectrum density. Note that the path-loss and shadowing-loss of transmission links between transmitter and distributed antennas are neglected. After CP removal, $r_{q,n_r}(n)$ is transformed into frequency domain by $N_c$-point DFT, yielding the frequency-domain received signal vector at the $n_r$-th distributed antenna and the $q$-th timeslot $\mathbf{R}_{q,n_r} = [R_{q,n_r}(0), R_{q,n_r}(1), \ldots, R_{q,n_r}(N_c-1)]^T$ as

$$R_{q,n_r}(k) = \sqrt{\frac{2E_s}{T_s}} \sum_{n_t=0}^{N_t-1} H_{n_r,n_t}(k)\, \widetilde{S}_{q,n_t}(k) + Z_{q,n_r}(k), \quad (10)$$

where $\widetilde{S}_{q,n_t}(k)$ is an element at the $k$-th frequency index of the frequency-domain transmit signal vector $\widetilde{\mathbf{S}}_{q,n_t}$ in (4). The frequency-domain channel response between $n_t$-th transmit antenna and the $n_r$-th distributed antenna and noise at the $n_r$-th distributed antenna and the $q$-th timeslot are expressed by

$$H_{n_r,n_t}(k) = \sum_{l=0}^{L-1} h_{n_r,n_t,l} \exp(-j2\pi k \tau_{n_r,n_t,l} / N_c), \quad (11a)$$

$$Z_{q,n_r}(k)=\frac{1}{N_c}\sum_{n=0}^{N_c-1} z_{q,n_r}(n)\exp(-j2\pi kn/N_c). \quad (11b)$$

FDE based on minimum mean-square error criterion (MMSE-FDE) is conducted by multiplying the MMSE weight matrix to the frequency-domain received matrix, then obtaining the equalized signal as $\widetilde{\mathbf{R}}_{(N_t\times Q)}=\mathbf{W}^H_{(N_t\times N_r)}\mathbf{R}_{(N_r\times Q)}$, where $\mathbf{W}=[\mathbf{W}_0,...,\mathbf{W}_{n_r},...,\mathbf{W}_{N_r-1}]$ and $\mathbf{W}_{n_r}=[\mathbf{W}_{n_r,0},...,\mathbf{W}_{n_r,n_t},...,\mathbf{W}_{n_r,N_t-1}]^T$ represents the MMSE-FDE weight matrix. The FDE weight at the $k$-th frequency index assuming SRRC transmit filtering with $\alpha$=0 is expressed by [2, 11].

$$W_{n_r,n_t}(k)=\frac{H_{n_r,n_t}(k)}{(\sum_{n_r=0}^{N_r-1}\sum_{n_t=0}^{N_t-1}|H_{n_r,n_t}(k)|^2)/N_t+(E_s/N_0)^{-1}}. \quad (12)$$

After that, STTD decoding is carried out in order to achieve spatial diversity gain. The frequency-domain decoded vector $\hat{\mathbf{X}}_j$, $j$=0~$J$−1 is obtained by the following STTD decoders [12], which employ only addition, subtraction and complex-conjugate operations on $\widetilde{\mathbf{R}}_{q,n_t}$ where $\widetilde{\mathbf{R}}_{q,n_t}$ is the matrix element in $\widetilde{\mathbf{R}}$:

$$\hat{\mathbf{X}}_{N_t=1}=\widetilde{\mathbf{R}}_{0,0}, \quad (13a)$$

$$\hat{\mathbf{X}}_{N_t=2}=\begin{bmatrix}\hat{\mathbf{X}}_0\\ \hat{\mathbf{X}}_1\end{bmatrix}=\begin{bmatrix}\widetilde{\mathbf{R}}_{0,0}+\widetilde{\mathbf{R}}^*_{1,1}\\ \widetilde{\mathbf{R}}_{0,1}-\widetilde{\mathbf{R}}^*_{1,0}\end{bmatrix}, \quad (13b)$$

$$\hat{\mathbf{X}}_{N_t=3}=\begin{bmatrix}\hat{\mathbf{X}}_0\\ \hat{\mathbf{X}}_1\\ \hat{\mathbf{X}}_2\end{bmatrix}=\begin{bmatrix}\widetilde{\mathbf{R}}_{0,0}+\widetilde{\mathbf{R}}^*_{1,1}+\widetilde{\mathbf{R}}^*_{2,2}\\ \widetilde{\mathbf{R}}_{0,1}-\widetilde{\mathbf{R}}^*_{1,0}+\widetilde{\mathbf{R}}^*_{3,2}\\ \widetilde{\mathbf{R}}_{0,2}-\widetilde{\mathbf{R}}^*_{2,0}-\widetilde{\mathbf{R}}^*_{3,1}\end{bmatrix}, \quad (13c)$$

$$\hat{\mathbf{X}}_{N_t=4}=\begin{bmatrix}\hat{\mathbf{X}}_0\\ \hat{\mathbf{X}}_1\\ \hat{\mathbf{X}}_2\end{bmatrix}=\begin{bmatrix}\widetilde{\mathbf{R}}_{0,0}+\widetilde{\mathbf{R}}^*_{1,1}+\widetilde{\mathbf{R}}^*_{2,2}+\widetilde{\mathbf{R}}_{3,3}\\ \widetilde{\mathbf{R}}_{0,1}-\widetilde{\mathbf{R}}^*_{1,0}-\widetilde{\mathbf{R}}_{2,3}+\widetilde{\mathbf{R}}^*_{3,2}\\ \widetilde{\mathbf{R}}_{0,2}+\widetilde{\mathbf{R}}_{1,3}-\widetilde{\mathbf{R}}^*_{2,0}-\widetilde{\mathbf{R}}^*_{3,1}\end{bmatrix}. \quad (13d)$$

Here, the discussion on the relationship between the phase rotation procedure in TD-SLM and the STTD decoder in (13) should be provided. Assuming $N_t$=2 and high received signal-to-noise power ratio (SNR), the frequency-domain signal vector after STTD decoding can be expressed by

$$\begin{aligned}\hat{\mathbf{X}}_{N_t=2} &= \begin{bmatrix}\widetilde{\mathbf{R}}_{0,0}+\widetilde{\mathbf{R}}^*_{1,1}\\ \widetilde{\mathbf{R}}_{0,1}-\widetilde{\mathbf{R}}^*_{1,0}\end{bmatrix}\\ &\approx \begin{bmatrix}\left(\sum_{n_r=0}^{N_r-1}\sum_{n_t=0}^{N_t-1}\mathbf{H}_{n_r,n_t}\mathbf{W}_{n_r,n_t}\mathbf{W}^H_{n_r,n_t}\mathbf{H}^H_{n_r,n_t}\right)\mathbf{X}_0\\ \left(\sum_{n_r=0}^{N_r-1}\sum_{n_t=0}^{N_t-1}\mathbf{H}_{n_r,n_t}\mathbf{W}_{n_r,n_t}\mathbf{W}^H_{n_r,n_t}\mathbf{H}^H_{n_r,n_t}\right)\mathbf{X}_1\end{bmatrix}.\end{aligned} \quad (14)$$

By referencing (3), (13) and (14), it is observed that the phase rotation is applied before DFT and STTD encoding, and will be removed after STTD decoding and IDFT. This indicates that the phase rotation in TD-SLM is independent from STTD coding, i.e. the input signal of STTD encoder and the output signal of STTD decoder are the phase-rotated signal. Since the phase rotation and STTD encoding are independent, STTD code orthogonality can be preserved even though $\mathbf{P}_{\hat{u},j}$ is not identical for all $j$=0~$J$−1. Note that the above observation is available only in transmission without transmit FDE.

After STTD decoding, $J$ blocks of the frequency-domain signal are then transformed back into time domain by $N_c$-point IDFT, yielding the $j$-th block of time-domain vector before de-mapping $\hat{\mathbf{x}}_j=[\hat{x}_j(0),\hat{x}_j(1),...,\hat{x}_j(N_c-1)]^T$, $j$=0~$J$−1 as

$$\hat{\mathbf{x}}_j=\mathbf{F}^H_{N_c}\hat{\mathbf{X}}_j\approx\sqrt{\frac{2E_s}{T_s}}\mathbf{F}^H_{N_c}\left(\sum_{n_r=0}^{N_r-1}\sum_{n_t=0}^{N_t-1}\mathbf{H}_{n_r,n_t}\mathbf{W}_{n_r,n_t}\mathbf{W}^H_{n_r,n_t}\mathbf{H}^H_{n_r,n_t}\right)\mathbf{X}_j. \quad (15)$$

Note that there still exists the phase rotation regarding to TD-SLM in $\hat{\mathbf{x}}_j$.

### 3.2. Joint blind phase rotation pattern estimation and data detection

In order to obtain the received symbol vector $\hat{\mathbf{d}}=[\hat{\mathbf{d}}_0,\hat{\mathbf{d}}_1,...,\hat{\mathbf{d}}_{J-1}]^T$, $j$=0~$J$−1 in the conventional transmission using TD-SLM technique, the time-domain received vector after STTD decoding $\hat{\mathbf{x}}_j$, $j$=0~$J$−1 is typically de-mapped (i.e. phase rotation removal) by multiplying with the Hermitian transpose of phase rotation matrix, that is

$$\hat{\mathbf{d}}=\mathbf{P}^H_{\hat{u}}\hat{\mathbf{x}}=\begin{bmatrix}\mathbf{P}^H_{\hat{u},0} & & & \mathbf{0}\\ & \mathbf{P}^H_{\hat{u},1} & & \\ & & \ddots & \\ \mathbf{0} & & & \mathbf{P}^H_{\hat{u},J-1}\end{bmatrix}\begin{bmatrix}\hat{\mathbf{x}}_0\\ \hat{\mathbf{x}}_1\\ \vdots\\ \hat{\mathbf{x}}_{J-1}\end{bmatrix}. \quad (16)$$

However, side-information sharing is needed for the signal detection technique in (16).

Joint blind phase rotation pattern estimation and data detection has been studied for SLM techniques in both OFDM [13] and SC-FDE [9-10], and has been extended to SC-FDE using STTD and FD-SLM [11]. In this paper, the phase rotation pattern estimation and data detection for TD-SLM in [10] is used and extended for SC-FDE using STTD. The joint blind phase rotation pattern estimation and data detection is carried out by generating the time-domain received candidates regarding to the $j$-th received block and the $v$-th phase rotation pattern $\mathbf{x}^{demap}_{j,v}=[x^{demap}_{j,v}(0),...,x^{demap}_{j,v}(N_c-1)]^T$ as

$$\mathbf{x}^{demap}_{j,v}=\mathbf{P}^H_{v,j}\hat{\mathbf{x}}_j, \quad (17)$$

where $j$=0~$J$−1 and $v$=0~$U$−1. $\mathbf{x}^{demap}_{v,j}$ is generated for all possible $U$ de-mapping patterns.

We know from [9-11] that $\mathbf{x}^{demap}_{j,\hat{u}}$ and $\mathbf{x}^{demap}_{j,v}$ are different and noticeable when $v\neq\hat{u}$ if the polyphase rotations are carried out in the TD-SLM. The time-domain received symbols $\mathbf{x}^{demap}_{j,v}{}_{j}$ where $v=\hat{u}$ are concentrated at the original signal constellations (assuming high SNR). On the other hand, the received symbols become

dispersive when $v \neq \hat{u}$. We can distinguish the received symbols with correct de-mapping by employing the maximum-likelihood (ML) signal detection as

$$\hat{\mathbf{d}}_j = \min_{\substack{v=0,1,\ldots,U-1,\\ \hat{d}_j(n)\in\Psi_{\mathrm{mod}}}} \frac{1}{N_c}\sum_{n=0}^{N_c-1}\left|x_{j,v}^{demap}(n)-\hat{d}_j(n)\right|^2, \quad (18)$$

where $\mathbf{r}_{j,v}^{demap}$ is defined in (17) and $\Psi_{\mathrm{mod}}$ is a set of original signal constellations for each modulation level. Note that the selected phase rotation pattern is also estimated simultaneously with data detection, but the information of phase rotation pattern is not used. In addition, if the TD-SLM is conduced based on the minimax criterion in (6), the ML-based detection in (18) can be carried out for $J$ received blocks simultaneously, and is rewritten as

$$[\hat{\mathbf{d}}_0,\ldots,\hat{\mathbf{d}}_{J-1}] = \min_{\substack{v=0,1,\ldots,U-1,\\ \hat{d}_j(n)\in\Psi_{\mathrm{mod}}}} \frac{1}{JN_c}\sum_{j=0}^{J-1}\sum_{n=0}^{N_c-1}\left|x_{j,v}^{demap}(n)-\hat{d}_j(n)\right|^2. \quad (19)$$

## 4. Performance Evaluation

Numerical and simulation parameters are summarized in Table 2. Channel coding is not considered. A set of phase rotation patterns is generated in random approach from polyphase rotations $\{e^{j0}, e^{j(2\pi/3)}, e^{-j(2\pi/3)}\}$. Note that the above polyphase rotations are not optimal but sufficient for allowing blind TD-SLM. In case of transmission with side-information sharing, the required side-information bits without channel coding are $J\log_2 U$ [8]. Performance of low-PAPR filtered SC-FDE using STTD and blind TD-SLM is shown in terms of PAPR and BER.

**Table 2** Simulation parameters.

| | | |
|---|---|---|
| **Transmitter** | Data modulation | 16QAM |
| | No. of subcarriers | $N_c$ = 256 |
| | CP length | $N_g$ = 16 |
| | Transmit filtering | SRRC ($\alpha$ = 0) |
| **SLM parameters** | SLM algorithm | TD-SLM |
| | Phase-rotation sequence type | Random polyphase |
| | No. of patterns | $U$ = 1(no SLM)~512 |
| | Oversampling factor | $V$ = 8 |
| **Channel** | Fading | Frequency-selective block Rayleigh |
| | Power delay profile | Symbol-spaced, 16-path uniform |
| **Receiver** | Channel estimation | Ideal |
| | FDE | Joint MMSE-FDE & STTD decoding |

### 4.1. $PAPR_{0.1\%}$

PAPR performance is evaluated by measuring the PAPR value at complementary cumulative distribution function (CCDF) equals $10^{-3}$, called $PAPR_{0.1\%}$, where its definition is $prob(\mathrm{PAPR}(\mathbf{s}) \geq \mathrm{PAPR}_{0.1\%}) = 10^{-3}$.

Fig. 3 shows the $PAPR_{0.1\%}$ of filtered SC-FDE using STTD and blind TD-SLM as a function of number of phase rotation patterns $U$. The $PAPR_{0.1\%}$ of blind TD-SLM and blind FD-SLM assuming $N_t$=1 are also shown for comparison. It is obviously seen from Fig. 3 that PAPR reduces when $U$ increases, which is consistent with the performance of blind TD-SLM in [10]. An increasing of $U$ results in an increasing of probability of obtaining low-PAPR transmit candidates.

It is also observed from Fig. 3 that $PAPR_{0.1\%}$ increases as $N_t$ increases when the phase rotation pattern is selected based on minimax criterion in (6), i.e. $PAPR_{0.1\%}$ increases by 0.4 dB and 0.6 dB when $N_t$ is 2 and 3, respectively. The reason is the minimax criterion decreases the degree of freedom in candidate generation in TD-SLM, and hence cannot guarantee an optimal solution for each transmit antenna. On the other hand, $PAPR_{0.1\%}$ does not increase when $N_t$ increases if the phase rotation pattern is selected based on (7), i.e. phase rotation pattern is selected in order to minimize the PAPR of each time-domain transmit block before STTD encoding $\mathbf{d}_j$. This makes the TD-SLM using the selection criterion in (7) become more attractive than the criterion in (6). In addition, the blind TD-SLM, with regardless of the selection criterion, achieves lower PAPR compared to that of single-antenna SC-FDE using FD-SLM.

### 4.2. BER performance

Figs. 4(a) and 4(b) show the BER performances of the proposed low-PAPR filtered SC-FDE using STTD and blind TD-SLM as a function of average total transmit bit energy-to-noise power spectrum density ratio $E_b/N_0=(1/N_{\mathrm{mod}})(E_s/N_0)(1+N_g/N_c)$ where $N_{\mathrm{mod}}$ represents modulation level (4 for 16QAM) assuming $N_t$=2 and 3, respectively. BER performances of transmission using TD-SLM with ideal side-information sharing are also plotted for comparison. The selection criterion of phase rotation patterns is organized by referring (7). The number of candidates is selected so as to achieve 3 dB of $PAPR_{0.1\%}$ reduction compared to conventional SC-FDE, that is $U$=256. Channel coding is not considered in this paper.

It is seen from Figs. 4(a) and 4(b) that the BER improves in both the low-PAPR filtered SC-FDE using STTD with TD-SLM with side-information sharing and blind TD-SLM when either $N_t$ or $N_r$ increases due to an increasing of spatial diversity gain. The BER performance of the low-PAPR filtered SC-FDE using STTD and blind TD-SLM degrades compared to the TD-SLM with ideal side-information sharing when the transmit power is low. This performance is also consistent with [10], where the reason is described as the noise enhancement and residual ISI makes the time-domain received signal vector becomes dispersive even though the de-mapping is carried out correctly. However, there is no difference on BER performances of transmission using the blind TD-SLM and that of the transmission using TD-SLM with ideal side-information sharing when the transmit power is high.

## 5. Conclusion

In this paper, the low-PAPR filtered SC-FDE using STTD and blind TD-SLM was proposed. Spatial diversity is achieved by employing orthogonal STBC. The use of polyphase rotations in TD-SLM allows signal detection without side-information. The proposed blind TD-SLM is implemented by employing phase rotation to the time-domain transmit block before STTD encoding. Computer simulation results confirmed that the proposed filtered SC-FDE using STTD and blind TD-SLM achieves low-PAPR without causing significant BER performance degradation, similar to the single-antenna case.


## Acknowledgement

This research was funded by the national project of "Research and Development on 5G mobile communications system" (#0155-0171, Sept. 2015), supported by the Ministry of Internal Affairs and Communications (MIC), Japan.


## References


[1] F. Adachi, K. Takeda, T. Yamamoto, R. Matsukawa and S. Kumagai, "Recent Advances in Single-Carrier Distributed Antenna Network," *Wiley Wireless Commun. and Moblie Comput.*, Vol. 11, pp. 1551-1563, Dec. 2011.

[2] S. M. Alamouti, "A simple transmit diversity technique for wireless communications," *IEEE J. Select. Areas. Commun.*, Vol. 16, No. 8, pp. 1451-1458, Oct. 1998.

[3] J. R. Hampton, *Introduction to MIMO Communications*, Cambridge University Press, 2013.

[4] D. Falconer, S. L. Ariyavisitakul, A. Benyamin-Seeyar and B. Edison, "Frequency Domain Equalization for Single-Carrier Broadband Wireless Systems," *IEEE Commun. Mag.*, Vol. 40, No. 4, pp. 58-66, Apr. 2002.

[5] A. Goldsmith, *Wireless Communications*, Cambridge University Press, 2005.

[6] Y. Akaiwa, *Introduction to Digital Mobile Communication*, 1st ed., Wiley, 1997.

[7] S. Okuyama, K. Takeda and F. Adachi, "MMSE Frequency-domain Equalization using Spectrum Combining for Nyquist Filtered Broadband Single-Carrier Transmission," *in Proc. IEEE Veh. Technol. Conference (VTC 2010-Spring)*, Taipei, Taiwan, May 2010.

[8] R. W. Bauml, R. F. H. Fischer and J. B. Huber, "Reducing the Peak-to-Average Power Ratio of Multicarrier Modulation by Selected Mapping," *IEEE Electron. Lett.*, Vol. 32, No. 22, pp. 2056-2057, Oct. 1996.

[9] A. Boonkajay and F. Adachi, "A Blind Selected Mapping Technique for Low-PAPR Single-Carrier Signal Transmission," *to be presented in Int. Conference on Inform. Commun. and Signal Process. (ICICS2015)*, Singapore, Dec. 2015.

[10] A. Boonkajay and F. Adachi, "Time-Domain Selected Mapping with Polyphase Rotations and Blind Detection for Filtered Single-Carrier Signals," *IEICE Tech. Rep. on Radio Commun. Syst. (RCS)*, RCS2015-160, pp. 101-106, Oct. 2015.

[11] A. Boonkajay and F. Adachi, "Frequency-Domain Blind Selected Mapping Technique for Space-Time Block Coded Low-PAPR SC-FDE," *IEICE Tech. Rep. on Radio Commun. Syst. (RCS)*, RCS2015-261, pp. 103-108, Dec. 2015.

[12] G. Ganesan and P. Stoica, "Space-time block codes: A maximum SNR approach," *IEEE Trans. Inform. Theory*, Vol. 48, No. 2, pp. 1650–1656, Apr. 2001.

[13] A. D. S. Jayalath and C. Tellambura, "SLM and PTS Peak Power Reduction of ODFM Signal without Side Information," *IEEE Trans. Wireless Commun.*, Vol. 4, No. 5, pp. 2006-2013, Sept. 2005.


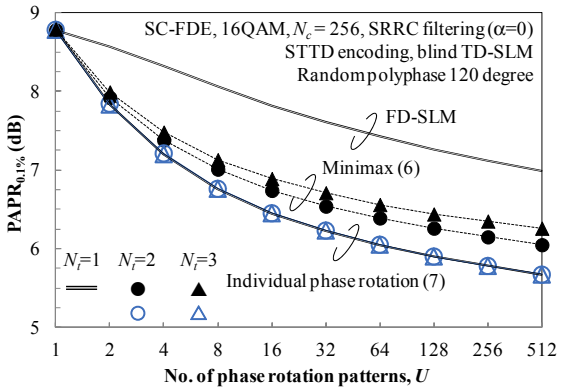


**Fig.3** $PAPR_{0.1\%}$ versus the number of candidates.

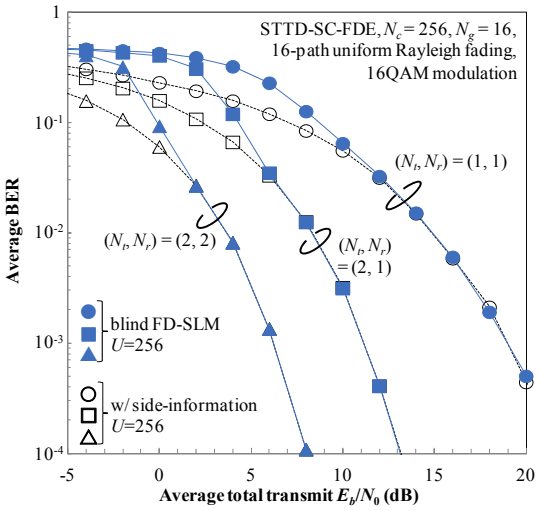


(a) 2 transmit antennas

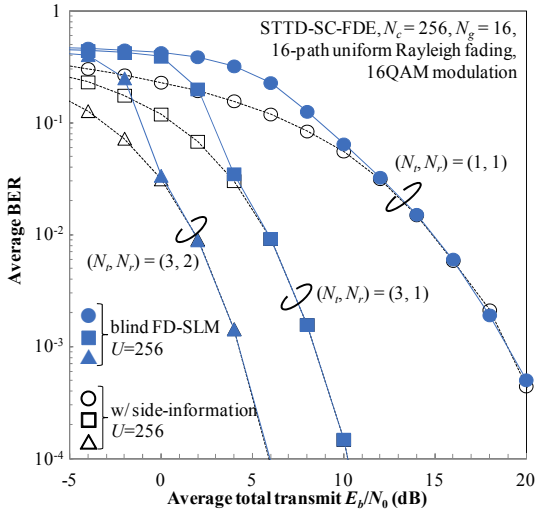


(b) 3 transmit antennas

**Fig.4** BER performances.